Hybridization model for a pair of intermediate valence manganese impurities

1998 J. Phys.: Condens. Matter 10 10249

(http://iopscience.iop.org/0953-8984/10/45/012)

J. Phys.: Condens. Matter **10** (1998) 10249–10261. Printed in the UK PII: S0953-8984(98)93214-3

Hybridization model for a pair of intermediate valence manganese impurities

P Schlottmann

Department of Physics, Florida State University, Tallahassee, FL 32306, USA

Received 9 April 1998, in final form 31 August 1998

Abstract. Manganese ions in a mixed-valent state of two magnetic configurations, Mn^{4+} and Mn^{3+}, play an important role in the magnetoresistance of $LaMnO_3$-based systems. We describe each Mn impurity with the Mn^{4+} represented by a spin $S = 3/2$ (three localized d electrons in the t_{2g} orbitals with their spins ferromagnetically coupled) and the Mn^{3+} configuration having an additional localized d electron in one of the e_g orbitals to form a total spin $(S + 1/2)$. The e_g electron hybridizes with the conduction electrons and the multiple occupancy of the e_g level is excluded by a large Coulomb energy at each site. This gives rise to a quadrupolar Kondo effect, which compensates the orbital degrees of freedom into a quadrupolar singlet, and interferes with the usual spin Kondo effect. We consider a pair of such manganese ions and allow the e_g electrons to hop between the two sites. Hence, bonding and antibonding levels are formed giving rise to the ferromagnetic double-exchange mechanism. We study the interaction between the impurities in the integer-valent and the mixed-valent regimes. In the integer-valent limit we renormalize the interactions using the vertex function in the leading logarithmic approximation. Two neighbouring impurities with the same integer valence interact ferromagnetically. Mn^{3+} ions have in addition a quadrupolar Kondo effect. In the intermediate valence regime we calculate the ground state energy, the valence, the population difference between the bonding and antibonding states, the charge susceptibility, the quadrupolar susceptibility and the response to a charge imbalance between the two sites as a function of the energy of the e_g level in zero magnetic field and for the spin-polarized limit (ferromagnetic lattice) using a mean-field slave-boson formulation. The results indicate that the intersite hopping suppresses charge order and lattice distortions.

1. Introduction

The discovery of the colossal magneto-resistance (CMR) in $La_{0.67}Ca_{0.33}MnO_3$ films [1] renewed the interest in the compounds of the $LaMnO_3$ family [2, 3]. The CMR is a collective phenomenon of a lattice of Mn atoms, which occurs close to the metal–insulator and para-/ferromagnetic transitions of the compounds. Charge order and coupling to the lattice, either in the form of polarons or the Jahn–Teller effect, have been found [4–6]. The lattice distortions manifest themselves in changes of the Mn–O bond lengths and angles, i.e. in local quadrupolar distortions in an otherwise cubic environment [7]. Most attempts to theoretically explain the phenomenon invoke the double-exchange mechanism [8].

The manganese ions exist in a mixed tri-/tetravalent state in which each of the three t_{2g} orbitals is singly occupied with their spins coupled to form a total spin $S = 3/2$. The e_g orbitals, on the other hand, are empty for Mn^{4+} and occupied by one 3d electron in Mn^{3+}, which is ferromagnetically correlated with the localized t_{2g} electrons. The intermediate

0953-8984/98/4510249+13$19.50

valence character of the Mn ions arises from the e_g electron, which may be localized at the Mn ion or become an itinerant electron either via hopping or hybridization [9]. A local change in the Mn–O bond lengths and angles corresponds to a lifting of the degeneracy of the two e_g levels (quadrupolar crystalline field).

In previous papers we studied the partial aspect of an isolated Mn impurity embedded into a crystal represented by a band of conduction electrons [10–13]. The single-impurity problem could be an important step toward the understanding of the full lattice problem. Studying the charge and quadrupolar susceptibilities we found that due to the interplay of the quadrupolar and spin Kondo effects [12] the spin-polarized (ferromagnetic) lattice is more favourable for charge order and lattice distortions than the paramagnetic electron gas [13]. The single-impurity problem lacks one key aspect of the manganites, namely the direct hopping of the e_g electrons between the Mn ions, which is the basis of the double-exchange mechanism [14].

In this paper we extend our results for an isolated Mn impurity to a pair of impurities embedded in a crystal represented by a band of conduction electrons. This allows us to study directly the interplay of the double-exchange mechanism (arising from the hopping matrix element for the e_g electrons between the ions) with the quadrupolar Kondo effect. We consider (i) the case of two integer-valent impurities and (ii) the situation of two mixed-valent impurities. Both regimes are important because the dominant mechanisms of interaction are different. Integer-valent impurities interact via the Ruderman–Kittel–Kasuya–Yosida (RKKY) interaction, while in the mixed-valent regime via the double-exchange mechanism. Close to integer valence there is a crossover region where both mechanisms have comparable magnitudes.

The rest of the paper is organized as follows. In section 2 we introduce the two-impurity model and summarize the results obtained for an isolated impurity. In section 3 we analyse the intersite interaction between the impurities in the integer-valent regime. This interaction is of the RKKY type with renormalized coupling parameters and is ferromagnetic at short distances if the Mn ions have the same integer valence. In section 4 we study the intersite interaction between the impurities in the mixed-valent regime. In this limit the double-exchange mechanism dominates over the RKKY exchange. Using a mean-field slave-boson approach we calculate the ground state energy, the valence, the occupation of the bonding and antibonding levels, the charge and quadrupolar susceptibilities and the response function for a charge imbalance between the two impurities in zero magnetic field and for the ferromagnetic lattice. Conclusions follow in section 5.

2. Model and results for an isolated impurity

2.1. Two-impurity model

The model under consideration is [12, 15, 16]

$$\begin{aligned} H = &\sum_{\boldsymbol{k}m\sigma} \epsilon_{\boldsymbol{k}} c^{\dagger}_{\boldsymbol{k}m\sigma} c_{\boldsymbol{k}m\sigma} + \epsilon_{e_g} \sum_{jM^*m} |jS^*M^*m\rangle\langle jS^*M^*m| \\ &+V \sum_{\boldsymbol{k}j\sigma mMM^*} (SM, \tfrac{1}{2}\sigma|S\tfrac{1}{2}S^*M^*)[\exp(\mathrm{i}\boldsymbol{k}\cdot\boldsymbol{R}_j)c^{\dagger}_{\boldsymbol{k}m\sigma}|jSM\rangle\langle jS^*M^*m| + \mathrm{HC}] \\ &-t \sum_{m\sigma M_1M_2M_1^*M_2^*} (SM_1, \tfrac{1}{2}\sigma|S\tfrac{1}{2}S^*M_1^*)(SM_2, \tfrac{1}{2}\sigma|S\tfrac{1}{2}S^*M_2^*) \\ &\times\{|1SM_1\rangle\langle 1S^*M_1^*m||2S^*M_2^*m\rangle\langle 2SM_2| + \mathrm{HC}\}. \end{aligned} \tag{1}$$

The first term is the kinetic energy of the conduction electrons and $m = +, -$ labels the two orbital channels with e_g symmetry. The impurities are labelled with $j = 1, 2$, and the bra and ket denote the impurity states. The states of the Mn^{4+} configuration are represented by a spin S (=3/2) and z-projection M, arising from three singly occupied t_{2g} orbitals with their spins coupled ferromagnetically (first Hund rule). The states of the Mn^{3+} configuration, on the other hand, have in addition one e_g orbital occupied, which is ferromagnetically correlated with the localized t_{2g} electrons to form a total spin $S^* = S + \frac{1}{2}$ with spin projection M^*. The Mn^{3+} states have in addition a label m to indicate which of the e_g states is occupied. The energy difference between the Mn^{3+} and Mn^{4+} configurations relative to the Fermi level is ϵ_{e_g}. The hybridization amplitude V and the hopping matrix element t allow for transitions between the two configurations. This gives rise to the intermediate valence character of the Mn ions. The Clebsch–Gordan coefficients select the spin components and are needed to preserve the spin rotational invariance. The completeness condition for the impurity states requires

$$\sum_{M^*m} |jS^*M^*m\rangle\langle jS^*M^*m| + \sum_{M} |jSM\rangle\langle jSM| = 1. \tag{2}$$

Note that the model excludes the multiple occupancy of the e_g levels, which can only be empty or occupied by one electron at each site. This corresponds to an implicit infinite on-site Coulomb repulsion.

2.2. Results for an isolated integer-valent impurity

In this subsection we summarize our results for isolated impurities in the integer-valent limits Mn^{4+} and Mn^{3+}. Impurities are isolated if $t = 0$ and $R = |\boldsymbol{R}_i - \boldsymbol{R}_j| \to \infty$. The integer-valent limits are obtained via a Schrieffer–Wolff transformation, which eliminates the hybridization term at the expense of higher order interaction terms [12].

For a tetravalent Mn impurity the Schrieffer–Wolff transformation leads to the following exchange interaction ($\epsilon_{e_g} \gg 0$, the impurity states are $|SM\rangle$)

$$H^{4+}_{exch} = -\frac{V^2}{|\epsilon_{e_g}|} \sum_{\boldsymbol{k}\boldsymbol{k}'\sigma\sigma' mMM'} \left[\frac{S+1}{2S+1} \delta_{\sigma\sigma'}\delta_{MM'} + \frac{2}{2S+1} \boldsymbol{S}_{MM'} \cdot \boldsymbol{s}_{\sigma\sigma'} \right] c^{\dagger}_{\boldsymbol{k}m\sigma} c_{\boldsymbol{k}'m\sigma'} |SM\rangle\langle SM'| \tag{3}$$

where the first term represents the identity and the second term a ferromagnetic spin exchange. Note that the interaction is diagonal in the orbital channel m. The electron–hole excitations in the electron gas give rise to logarithmic terms in the vertex function. Within the leading logarithmic approximation the two vertex amplitudes renormalize to

$$\Gamma^0(\omega) = -\frac{(S+1)V^2}{(2S+1)|\epsilon_{e_g}|} \qquad \Gamma^s(\omega) = -\frac{V^2/|\epsilon_{e_g}|}{1 + [2V^2\rho/(2S+1)|\epsilon_{e_g}|]\ln(D/|\omega|)} \tag{4}$$

where D is the cut-off for electronic excitations and the two amplitudes refer to the normal scattering and exchange, respectively. As $\omega \to 0$ the exchange vertex tends to zero, characteristic of the weak coupling regime and the asymptotic freedom of the impurity spin.

The Mn^{3+} integer-valent limit, on the other hand, renormalizes to a strong coupling fixed point, which corresponds to a Kondo effect in both the spin and orbital sectors. The Schrieffer–Wolff transformation yields four vertices, i.e. the trivial normal scattering amplitude and three nontrivial scattering amplitudes, namely, pure spin exchange ($\Gamma^s(\omega)$),

pure quadrupolar pseudospin exchange ($\Gamma^m(\omega)$) and a combined spin and quadrupolar exchange ($\Gamma^{sm}(\omega)$),

$$\tilde{\Gamma}(\omega) = \frac{1}{4}\Gamma^0(\omega)\hat{I}_m\hat{I}_s + \frac{1}{2S+1}\Gamma^s(\omega)\hat{I}_m(\boldsymbol{S}\cdot\boldsymbol{s}) + \Gamma^m(\omega)(\boldsymbol{T}\cdot\boldsymbol{\tau})\hat{I}_s + \frac{4}{2S+1}\Gamma^{sm}(\omega)(\boldsymbol{T}\cdot\boldsymbol{\tau})(\boldsymbol{S}\cdot\boldsymbol{s}). \tag{5}$$

Here $\boldsymbol{S}$ ($\boldsymbol{s}$) and $\boldsymbol{T}$ ($\boldsymbol{\tau}$) are spin and pseudospin (orbital channels) operators for the impurity (conduction electrons), and $\hat{I}_s$ and $\hat{I}_m$ are the identity operators in the spin and quadrupolar spaces, respectively. The operator $\boldsymbol{S}$ acts on the space of the spin S^*. The renormalization group equations for these amplitudes within the leading logarithmic order are [12]

$$\frac{\mathrm{d}\Gamma^0}{\mathrm{d}x} = 0 \qquad \frac{\mathrm{d}\Gamma^s}{\mathrm{d}x} = \frac{1}{2S+1}(\Gamma^s)^2 + \frac{3}{2S+1}(\Gamma^{sm})^2$$
$$\frac{\mathrm{d}\Gamma^m}{\mathrm{d}x} = (\Gamma^m)^2 + \frac{2S+3}{2S+1}(\Gamma^{sm})^2 \qquad \frac{\mathrm{d}\Gamma^{sm}}{\mathrm{d}x} = 2\Gamma^m\Gamma^{sm} + \frac{2}{2S+1}\Gamma^s\Gamma^{sm} \tag{6}$$

with $x = \ln(D/D')$, where D' is the cutoff after all excitated states of energy in the interval $D' < |\omega| < D$ have been eliminated.

Due to the interference between the orbital and spin Kondo effects the Kondo energy scale is a function of the magnetic field. For the spin-polarized impurity (ferromagnetic lattice) the characteristic energy scale is given by $T_K = D\exp(-1/\mathcal{J}\rho_F)$ independently of the spin S, where $\mathcal{J} = 2V^2/|\epsilon_{e_g}|$. In zero magnetic field the three coupled scattering amplitudes diverge at the same energy ω given by [12]

$$T_K^* = D\exp[-a(S)/(\mathcal{J}\rho_F)] \tag{7}$$

where $a(S)$ is a constant that depends on the spin. For $S = 0$ we obtain $a(0) = 0.5$ (SU(4) invariance), for $S \to \infty$ we have $a(\infty) = 1$ (classical spin, i.e. pure quadrupolar Kondo effect) and for $S = 3/2$ it is $a(3/2) = 0.8306$. The spin is compensated from $S^* = S + \frac{1}{2}$ to S via the spin Kondo effect and simultaneously the orbital exchange gives rise to an orbital singlet state via the quadrupolar Kondo effect. The ground state of the impurity is always magnetic for $S > 0$.

2.3. Results for an isolated mixed-valent impurity

For an isolated intermediate valence impurity we calculated [13] the ground state energy, the valence, and the charge and quadrupolar susceptibilities as a function of ϵ_{e_g} within (a) the saddle-point slave-boson formulation, (b) the non-crossing diagram approximation and (c) the Bethe *ansatz* (spin-polarized limit only). The quadrupolar crystalline field susceptibility is related to deviations of the Mn–O bond lengths and angles from their values in cubic symmetry, and to the response to local deformations due to the Jahn–Teller effect. The charge susceptibility (defined as $\chi_{charge} = -\partial^2 E_G/\partial\epsilon_{e_g}^2$, where E_G is the ground state energy) for the single impurity, on the other hand, is a measure for a possible charge order in a lattice of Mn ions (compound). For each case we compared the zero-magnetic-field case to the spin-polarized limit [13].

Both the mean-field slave-boson and the non-crossing diagram approximations are expansions in terms of the inverse of an effective degeneracy for the d electron with e_g symmetry [17]. The effective degeneracy arises from the interplay of the spin and quadrupolar Kondo effects and is the same for both approaches, $\mathrm{deg} = 2(2S+2)/(2S+1)$, but is slightly different from that obtained within the leading logarithmic order approach,

$N_{eff} = 2/a(S)$, where $a(S)$ is defined in equation (7). Both approaches also yield very similar results and the same trends.

The peak of the charge susceptibility increases with the magnetic field (consequence of the effective reduction of the degeneracy), indicating that the ferromagnetic state for the Mn lattice is more likely to have charge order than the zero-magnetic-field ground state. Also the quadrupolar response increases with increasing magnetic field, since the spin screening (spin undercompensation) is gradually broken up. As the spin compensation is broken up, the Kondo energy scale is reduced and hence χ_{quadr} enhanced. Hence, within the limitations of an impurity model, this result suggests that quadrupolar distortions of the Mn–O bond lengths are more favourable in the spin-polarized regime, i.e. close to or in the ferromagnetic regime of $LaMnO_3$ compounds, rather than in the paramagnetic phase.

3. RKKY interaction for integer-valent impurities

In this section we study the intersite interaction of two Mn impurities in the same integer-valent configuration. The hopping t between the sites does not play any role in this limit, since either all e_g levels are empty (Mn^{4+} ions) or both sites have exactly one e_g electron (Mn^{3+} ions). The interaction is then mediated by the conduction electrons and hence of the RKKY type.

Consider first two Mn^{4+} ions. The RKKY interaction is then given by

$$H_{int} = \frac{4mk_F^4}{(2\pi)^3}\left(\frac{2}{2S+1}\Gamma^s\right)^2 F(2k_F R)\boldsymbol{S}_1 \cdot \boldsymbol{S}_2 \tag{8}$$

where we assumed a parabolic band of effective mass m, k_F is the Fermi wavenumber, Γ^s is given by equation (4), R is the distance between the impurities and

$$F(x) = \frac{x\cos(x) - \sin(x)}{x^4}. \tag{9}$$

For short distances, i.e. small x, we have $F(x) \approx -1/(3x)$, so that for nearest neighbour sites and low carrier concentration the interaction is ferromagnetic. Since Γ^s is reduced in magnitude by the electron–hole excitations, the coupling between the impurities is expected to be weak.

The situation is more complicated for a pair of Mn^{3+} impurities, since there are three nontrivial vertices (see equation (5)). Tracing out the conduction electron degrees of freedom we obtain the expression

$$H_{int} = \frac{4mk_F^4}{(2\pi)^3}F(2k_F R)\left[\frac{1}{(2S+1)^2}(\Gamma^s)^2\hat{I}_m(\boldsymbol{S}_1^* \cdot \boldsymbol{S}_2^*) + (\Gamma^m)^2(\boldsymbol{T}_1 \cdot \boldsymbol{T}_2)\hat{I}_s\right] + \frac{4mk_F^4}{(2\pi)^3}F(2k_F R)\left[\frac{2}{(2S+1)^2}(\Gamma^{ms})^2(\boldsymbol{T}_1 \cdot \boldsymbol{T}_2)(\boldsymbol{S}_1^* \cdot \boldsymbol{S}_2^*)\right]. \tag{10}$$

This case corresponds to a strong coupling fixed point because the vertex functions all diverge at $|\omega| = T_K^*$. At short distances and low carrier concentration, $F(2k_F R) < 0$, so that the interaction between neighbouring ions is again 'ferromagnetic'.

In addition to the intersite interactions the quadrupolar Kondo effect, leading to a quadrupolar singlet at each site, has to be taken into account. Hence, the single-site and intersite interactions compete and cannot be satisfied simultaneously. The interplay of all these interactions gives rise to a non-universal behaviour, in which the spins are ferromagnetically coupled, but the quadrupolar pseudospins of the impurities are partially compensated into Kondo singlets and partially aligned with each other. The situation is

then similar to the two-impurity Kondo problem with ferromagnetic RKKY, but now for quadrupolar degrees of freedom: the global ground state is a quadrupolar singlet, which is formed in two steps, namely first the pseudospins 1/2 couple to a pseudospin 1, which is then compensated into a singlet by the conduction electrons [18].

The third situation that could be analysed is the interaction among two unlike integer-valent Mn ions. The RKKY interaction of one Mn^{3+} with one Mn^{4+} ion is antiferromagnetic at short distances. But in this case the e_g electron would be able to hop between the two sites giving rise to a strong ferromagnetic double-exchange mechanism. This mechanism is proportional to t and more important than the RKKY interaction (which is of order V^4).

4. Pair of impurities in the mixed-valent regime

4.1. Slave-boson formulation

We introduce slave-boson creation and annihilation operators [19] for the impurities, $b^\dagger_{jM}$ and b_{jM}, which act as projectors onto the corresponding impurity states of the Mn^{4+} configuration with spin component M at the site j. Similarly we introduce fermion creation and annihilation operators for the Mn^{3+} states at the site j, $d^\dagger_{jM^*m}$ and d_{jM^*m}. They satisfy the completeness relation [19]

$$\sum_M b^\dagger_{jM} b_{jM} + \sum_{M^*m} d^\dagger_{jM^*m} d_{jM^*m} = 1 \tag{11}$$

which is equivalent to the condition (2), i.e. that each impurity has to be in one and only one of the states of the Mn^{3+} and Mn^{4+} configurations. The operators describing the transitions between the configurations are rewritten as

$$|jSM\rangle\langle jS^*M^*m| = b^\dagger_{jM} d_{jM^*m} \tag{12}$$

and the Hamiltonian in terms of slave bosons is then

$$\begin{aligned} H = {} & \sum_{\boldsymbol{k}m\sigma} \epsilon_{\boldsymbol{k}} c^\dagger_{\boldsymbol{k}m\sigma} c_{\boldsymbol{k}m\sigma} + \epsilon_{e_g} \sum_{jM^*m} d^\dagger_{jM^*m} d_{jM^*m} \\ & + V \sum_{\boldsymbol{k}j\sigma mMM^*} (SM, \tfrac{1}{2}\sigma | S\tfrac{1}{2} S^* M^*)[\exp(\mathrm{i}\boldsymbol{k}\cdot\boldsymbol{R}_j) c^\dagger_{\boldsymbol{k}m\sigma} b^\dagger_{jM} d_{jM^*m} + \mathrm{HC}] \\ & - t \sum_{m\sigma M_1 M_2 M_1^* M_2^*} (SM_1, \tfrac{1}{2}\sigma | S\tfrac{1}{2} S^* M_1^*)(SM_2, \tfrac{1}{2}\sigma | S\tfrac{1}{2} S^* M_2^*) \\ & \times \{ d^\dagger_{1M_1^* m} b_{1M_1} b^\dagger_{2M_2} d_{2M_2^* m} + d^\dagger_{2M_2^* m} b_{2M_2} b^\dagger_{1M_1} d_{1M_1^* m} \} \end{aligned} \tag{13}$$

subject to the constraint (11), which restricts the model to the physical subspace.

The above slave-boson formulation is exact, i.e. it does not contain approximations with respect to the original two-impurity Hamiltonian, equation (1). The mean-field approximation for the slave-boson formulation has given qualitatively and even quantitatively reliable results for the single-impurity [20], two-impurity [21] and lattice [21–23] Anderson models. In the mean-field (saddle-point) approximation [20] we replace all boson operators by their expectation value, i.e. $\langle b_{jM}\rangle = \langle b^\dagger_{jM}\rangle = b$, where we assumed that both sites have the same valence. In zero magnetic field the ground state is $(2S+1)$-fold degenerate and all $b^\dagger_M$ operators have the same expectation value. The constraints (11) are incorporated via Lagrange multipliers λ_j. If the two impurities are assumed identical we have $\lambda_1 = \lambda_2$, so that the subindex can be dropped. It is useful to introduce states with even and odd parity about the midpoint between the impurities, i.e. with $P = \pm 1$, [21]

$$d_{PM^*m} = 2^{-1/2}(d_{1M^*m} + P d_{2M^*m}). \tag{14}$$

The hopping between sites is most effective if the two impurities are in the same state, i.e. $M_1^* = M_2^*$. The hopping amplitude between different states, i.e. $M_1^* \neq M_2^*$ is strongly reduced by the Clebsch–Gordan coefficients. It is a reasonable approximation for the ground state to keep only the largest hopping term and neglect all others. In terms of the parity states the mean-field Hamiltonian then takes the form

$$\begin{aligned} H_{mf} = &\sum_{\boldsymbol{k}m\sigma} \epsilon_{\boldsymbol{k}} c^\dagger_{\boldsymbol{k}m\sigma} c_{\boldsymbol{k}m\sigma} + \sum_{PM^*m} [\epsilon_{e_g} + \lambda - tb^2 P] d^\dagger_{PM^*m} d_{PM^*m} \\ &-2\lambda + 2\lambda(2S+1)b^2 + 2^{-1/2} Vb \sum_{\boldsymbol{k}P\sigma mMM^*} (SM, \tfrac{1}{2}\sigma | S\tfrac{1}{2} S^* M^*) \\ &\times \{c^\dagger_{\boldsymbol{k}m\sigma} [\exp(\mathrm{i}\boldsymbol{k}\cdot\boldsymbol{R}_1) + P\exp(\mathrm{i}\boldsymbol{k}\cdot\boldsymbol{R}_2)] d_{PM^*m} + \mathrm{HC}\}. \end{aligned} \tag{15}$$

The minimization of the ground state energy with respect to b and λ then yields

$$\begin{aligned} &2(2S+1)\lambda b - tb \sum_{PM^*m} P\langle n_{PM^*m}\rangle + 2^{-1/2} V \sum_{\boldsymbol{k}P\sigma mMM^*} (SM, \tfrac{1}{2}\sigma | S\tfrac{1}{2} S^* M^*) \\ &\quad \times [\exp(\mathrm{i}\boldsymbol{k}\cdot\boldsymbol{R}_1) + P\exp(\mathrm{i}\boldsymbol{k}\cdot\boldsymbol{R}_2)] \langle c^\dagger_{\boldsymbol{k}m\sigma} d_{PM^*m}\rangle = 0 \\ &1 = (2S+1)b^2 + \tfrac{1}{2} \sum_{PM^*m} \langle n_{PM^*m}\rangle. \end{aligned} \tag{16}$$

The expectation values $\langle d^\dagger_{PM^*m} d_{PM^*m}\rangle$ and $\langle c^\dagger_{\boldsymbol{k}m\sigma} d_{PM^*m}\rangle$ are obtained from the one-particle Green functions for the mean-field Hamiltonian. The Green functions involve the following expression [21]

$$\sum_{\boldsymbol{k}} \frac{1 - P\exp(\mathrm{i}\boldsymbol{k}\cdot\boldsymbol{R})}{z - \epsilon_{\boldsymbol{k}}} \approx -\mathrm{i}\pi\rho_F \left[1 + P\frac{\sin(k_F R)}{k_F R}\right] = -\mathrm{i}\pi\rho_F F_P \tag{17}$$

where R is the distance between the impurities and ρ_F is the density of states of the conduction electrons at the Fermi level. In equation (17) we carried out the angular integrations and then projected the energy onto the Fermi level [21]. The Green function for the e_g electron with quantum numbers P, M^* and m is then diagonal and involves a single resonance. The resonance width depends on the parity and is $\pi\rho_F V^2 b^2 F_P$. The mean-field relations then lead to the following transcendental equations

$$\begin{aligned} \tilde{\epsilon} &= \epsilon_{e_g} + \deg\frac{\Gamma}{2\pi} \sum_P F_P \ln\left(\frac{D}{\sqrt{(\tilde{\epsilon} - Ptb^2)^2 + (\Gamma b^2 F_P)^2}}\right) + \deg\frac{\Gamma}{4\pi} tb^2 \sum_P \frac{PF_P}{\tilde{\epsilon} - Ptb^2} \\ b^2 &= \frac{1}{(2S+1)} - \deg\frac{\Gamma}{2\pi} b^2 \sum_P \frac{F_P}{\tilde{\epsilon} - Ptb^2} \end{aligned} \tag{18}$$

where $\Gamma = \pi V^2 \rho_F$, $\tilde{\epsilon} = \epsilon_{e_g} + \lambda$ and deg is an effective degeneracy. The sum over the e_g levels and the Clebsch–Gordan coefficients leads then to $\deg = 2(2S+2)/(2S+1)$. Here we assumed that there is no external magnetic field. The 'small parameter' of this mean-field theory is the inverse of the degeneracy. The larger the degeneracy the smaller are the contributions from fluctuations about the saddle point (1/deg expansion) [20].

For the spin-polarized system, on the other hand, only $\langle b^\dagger_S\rangle$ is different from zero and the Clebsch–Gordan coefficient is just one, so that $\deg = 2$, arising from the two orbital degrees of freedom. Hence, the above results also hold for the ferromagnetic lattice if we set $\deg = 2$ and $S = 0$ (the total polarization quenches the spin).

4.2. Results

We assume now that the two impurities are very far apart, i.e. $F_P = 1$ and $t = 0$. For $\epsilon_{e_g} \ll 0$ we can neglect $\tilde{\epsilon}$ on the right-hand side of the first of equations (18) and obtain the characteristic energy scale (Kondo temperature) for an isolated impurity

$$T_K^* = D \exp[\pi \epsilon_{e_g} / \Gamma \deg] = D \exp[-a(S)/(\mathcal{J}\rho_F)] \tag{19}$$

where $a(S) = (2S + 1)/(2S + 2)$ in zero field and $a(S) = 1$ for the spin-polarized situation corresponding to an effective degeneracy $\deg = 2/a(S)$. The values of $a(S)$ obtained within the mean-field slave-boson approach (they are equal to those for the non-crossing diagram approximation) are slightly different from the ones generated by the renormalization group equations [12]. The energy scale arises from the interplay of the spin Kondo effect (undercompensated impurity) and the quadrupolar Kondo effect. Within the leading logarithmic approximation the renormalization group consists of three non-trivial amplitudes, while in mean-field approximation the T_K^* depends only on the parameters S and deg. An approach involving only one-particle Green functions (many-particle Green functions are factorized in mean field) cannot take into account the full many-body structure of the problem. However, the differences in the $a(S)$ is small and they agree in the limiting cases $S = 0$ and $S \to \infty$. On the other hand, for the spin-polarized system the energy scales are identical (pure quadrupolar Kondo effect).

We have solved equations (18) numerically and obtained the ground state energy $E_G = \epsilon_{e_g} - \tilde{\epsilon}$, the valence $n_d = 1 - (2S+1)b^2$ and the charge susceptibility $\chi_{charge} = -\partial n_d / \partial \epsilon_{e_g}$. These quantities as a function of ϵ_{e_g} are shown in figures 1(A)–1(C) and 2(A)–2(C) for $S = 3/2$ (zero magnetic field) and $S = 0$ (spin-polarized system), respectively. The band cutoff and the hybridization matrix element chosen for these figures are $D = 10$ and $V = 1$, and the four curves shown refer to (a) $t = 0$, $k_F R = \pi$, (b) $t = 0$, $k_F R = \pi/2$, (c) $t = 2$, $k_F R = \pi$ and (d) $t = 2$, $k_F R = \pi/2$. For $k_F R = \pi$ the resonance widths of the localized e_g electrons are the same for even and odd parity and equal to that of an isolated impurity. For $k_F R = \pi/2$, on the other hand, the states with even parity have a much broader resonance width than the states with odd parity. The hopping t gives rise to a splitting into bonding and antibonding states.

For $t = 0$ the ground state energy per Mn ion is essentially the same as for an isolated impurity, independent of the interference amplitude $\sin(k_F R)/(k_F R)$. If $t = 0$ the bonding and antibonding states have the same resonance energy and their tails in the density of states are occupied simultaneously. For finite t the bonding states (having lower energy) are occupied first and then are antibonding states. This, on the one hand, lowers the energy of the system and, on the other hand, substantially broadens the intermediate valence regime. This effect is larger in the spin-polarized limit because of the smaller effective degeneracy of the states (the spin is quenched). The value of b^2, which determines the valence, varies between 0 (Kondo limit) and $1/(2S + 1)$ (Mn^{4+} limit). The range of variation of the bonding–antibonding splitting (given by $2tb^2$) is then much larger for the ferromagnetic system, and consequently n_d against ϵ_{e_g} is much broader in this case. The rate of change of n_d with ϵ_{e_g} determines χ_{charge} and is shown in figures 1(C) and 2(C).

To determine the quadrupolar susceptibility χ_{quadr} we lift the degeneracy of the two e_g levels by a small quadrupolar field and obtain

$$\chi_{quadr} = (2S+1)\frac{\deg}{8\pi} \sum_P \frac{\Gamma b^2 F_P}{(\tilde{\epsilon} - P t b^2)^2}. \tag{20}$$

In the Kondo regime both b^2 and $\tilde{\epsilon}$ are proportional to T_K^*, so that $\chi_{quadr} \propto (T_K^*)^{-1}$. It is then convenient to display the logarithm of χ_{quadr} to explicitly show this behaviour (see

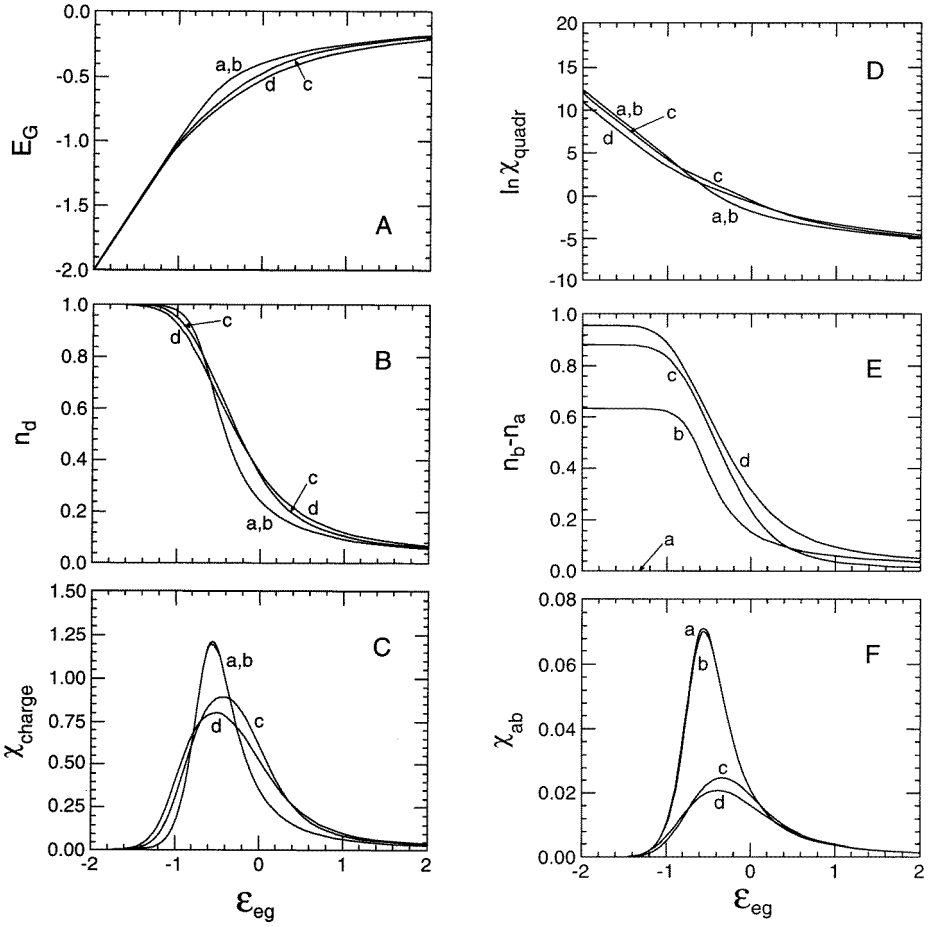

Figure 1. (A) Ground state energy, (B) number of localized e_g electrons, (C) charge susceptibility, (D) quadrupolar susceptibility, (E) population difference between bonding and antibonding states and (F) response function for charge imbalance between the two sites as a function of ϵ_{e_g} per Mn impurity with $D = 10$ and $V = 1$. The results were obtained within the mean-field slave-boson approach assuming no external magnetic field ($S = 3/2$ and deg $= 2.5$). Curves (a) correspond to $t = 0$ and $k_F R = \pi$, (b) to $t = 0$ and $k_F R = \pi/2$, (c) to $t = 2$ and $k_F R = \pi$ and (d) to $t = 2$ and $k_F R = \pi/2$.

figures 1(D) and 2(D)). If $t = 0$ the dependence of χ_{quadr} on ϵ_{e_g} is similar to the isolated impurity. Due to the smaller degeneracy the quadrupolar susceptibility for $t = 0$ in the Kondo regime is larger in the spin-polarized phase than in zero magnetic field. The large quadrupolar susceptibility in the Kondo limit is strongly reduced by the bonding–antibonding splitting $2tb^2$. For $t \neq 0$ the quadrupolar screening of the molecule takes place in two steps, defined by the constant slope segments in figures 1(D) and 2(D). As $\epsilon_{e_g} \to -\infty$ the relevant energy scale in each case is again T_K^*. From these results we conclude that the intersite hopping stabilizes the pair of impurities with respect to quadrupolar lattice distortions of the Jahn–Teller and small polaron type.

The population difference between the bonding and antibonding states is shown in figures 1(E) and 2(E). This difference is of course zero for $t = 0$ and $k_F R = \pi$ (curve (a)).

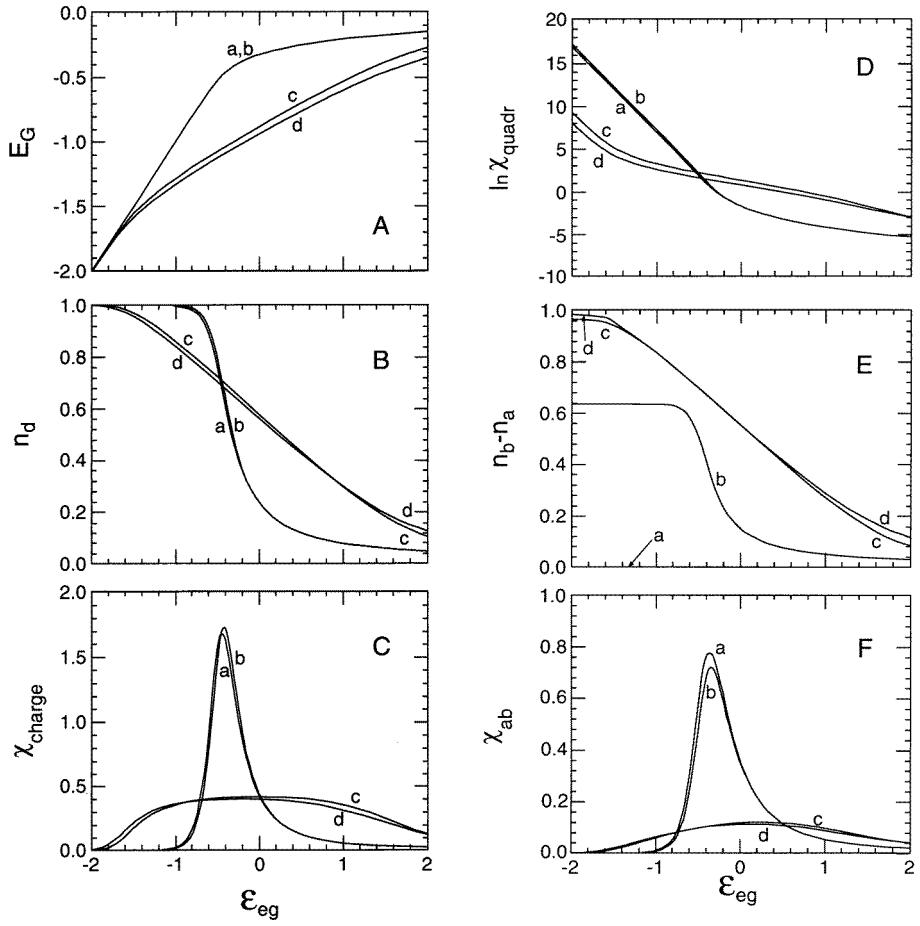

Figure 2. (A) Ground state energy, (B) number of localized e_g electrons, (C) charge susceptibility, (D) quadrupolar susceptibility, (E) population difference between bonding and antibonding states and (F) response function for charge imbalance between the two sites as a function of ϵ_{e_g} per Mn impurity with $D = 10$ and $V = 1$. The results were obtained within the mean-field slave-boson approach assuming a spin-polarized lattice ($S = 0$ and deg $= 2.0$). Curves (a) correspond to $t = 0$ and $k_F R = \pi$, (b) to $t = 0$ and $k_F R = \pi/2$, (c) to $t = 2$ and $k_F R = \pi$ and (d) to $t = 2$ and $k_F R = \pi/2$.

The difference is given by

$$n_b - n_a = (2S+1)\frac{\deg}{2\pi}\sum_P \frac{P\Gamma b^2 F_P}{\tilde{\epsilon} - Ptb^2} \tag{21}$$

and is largest in the Kondo regime where the width of the levels is smallest. The intermediate valence regime grows with t and is much more pronounced in curves (c) and (d), in particular for the spin-polarized system.

The response to a charge imbalance between the two sites, i.e. the two sites having different valence, corresponds to the bubble diagram consisting of one bonding and one antibonding propagator, i.e. the correlation function of $b^2 \sum_{mM^*} d^\dagger_{+M^*m} d_{-M^*m}$ with its

Hermitian conjugate, and is given by

$$\chi_{ab} = (2S+1)\frac{b^2 \mathrm{deg}\Gamma/(2\pi)}{t^2 + \Gamma^2[\sin(k_F R)/k_F R]^2} \times \sum_P P\left\{\frac{\sin(k_F R)}{2k_F R}\ln[(\tilde{\epsilon} - Ptb^2)^2 + (\Gamma b^2 F_P)^2] + \frac{tb^2 F_P}{\tilde{\epsilon} - Ptb^2}\right\}. \quad (22)$$

This correlation function vanishes in the integer-valent limits, because either there is already one electron per site or there is no electron to be transferred. The results are displayed in figures 1(F) and 2(F) as a function of ϵ_{e_g}. A charge imbalance is most favourable in the mixed-valent regime for $t = 0$ for the spin-polarized situation. The intersite hopping reduces χ_{ab} and stabilizes the charge. Charge order then becomes less favourable with growing t, but it is more likely in a ferromagnetic lattice.

5. Concluding remarks

We considered a pair of interacting integer-valent (trivalent and tetravalent) and intermediate valence Mn impurities with its ground state wavefunction being a linear superposition of the Mn^{3+} and Mn^{4+} configurations. In the manganites (cubic symmetry) the Mn^{4+} ions have three localized d electrons in the t_{2g} orbitals, while the Mn^{3+} configuration has an additional d electron with e_g symmetry. The first of Hund's rules couples all the d electrons ferromagnetically, maximizing the total spin of each impurity. The two configurations are mixed by the intersite hopping and the hybridization of the e_g orbitals with the conduction band. In zero magnetic field the ground state of each impurity is $(2S+1)$-fold degenerate because both configurations are magnetic.

Two situations have to be distinguished: (a) two integer-valent impurities of equal valence and (b) two intermediate valence ions. In the former case the hopping does not play any role; and the interaction mediated by the conduction states is of the RKKY type. For the latter situation the double-exchange mechanism dominates over the RKKY interaction. Close to integer valence there is a crossover between these two regimes where the two interactions have comparable strength. In the manganites, close to integer valence, the interaction is dominated by the superexchange mediated by the O^{2-} ions. This antiferromagnetic interaction is not considered in our simple model.

For two impurities with the same integer valence the intersite hopping t can be neglected. Mn^{4+} impurities are only weakly coupled to the electron gas and the amplitude of the RKKY interaction between two Mn^{4+} ions is then small. The situation is different for Mn^{3+} impurities, where the interaction with the electron gas corresponds to a strong coupling fixed point. This interaction leads to screening in both the spin and orbital channels, i.e. to a combined spin and quadrupolar Kondo effect. Within the leading logarithmic parquet approximation for the integer-valent limit (Mn^{3+}) the interaction is described in terms of four vertex amplitudes, namely a trivial normal scattering amplitude and three non-trivial ones. The latter ones correspond to a pure spin exchange, a pure quadrupolar exchange (the e_g levels are represented by an isospin) and a combined spin and orbital exchange interaction. All three exchange amplitudes diverge at the same energy, which defines T_K^*. The Kondo temperature depends on the exchange coupling in the usual exponential form, but with a coefficient $a(S)$ representing an effective degeneracy. For the spin-polarized situation the spin exchange is suppressed and a pure quadrupolar Kondo effect is obtained (only one non-trivial vertex) that leads to the orbital singlet. The RKKY interaction between neighbouring sites (assuming $k_F R$ small) is ferromagnetic for the spins. The single-site and intersite

interactions for the quadrupolar pseudospin compete and cannot be satisfied simultaneously. The interplay of all these interactions gives rise to non-universal behaviour, in which the quadrupolar pseudospins are partially compensated into Kondo singlets and partially aligned with each other. The situation is similar to the two-impurity (magnetic) Kondo problem with ferromagnetic RKKY: the global groundstate is a quadrupolar singlet, which is formed in two steps, namely first the pseudospins 1/2 couple to a pseudospin 1, which is then compensated into a singlet by the conduction electrons [18].

For the impurities in the intermediate valence regime we calculated the ground state energy, the valence, the charge susceptibility, the quadrupolar susceptibility, the population difference between the bonding and antibonding states and the response function for a charge imbalance between the two sites within the mean-field (saddle-point) slave-boson approach. This mean-field approximation is an expansion in terms of the inverse of an effective degeneracy for the d electron with e_g symmetry. In particular we focused on the interplay between the intersite hopping and the Kondo effect. The intersite hopping couples the two impurities ferromagnetically, as expected from the double-exchange mechanism [14]. The hopping t splits the impurity states into a bonding and an antibonding state. These correspond to states with even and odd parity with respect to the midpoint between the impurities. Bonding and antibonding states act similarly to two impurities with different d electron energy ϵ_{e_g} (the splitting). Hence, the corresponding d levels are populated at a different rate. This considerably broadens the intermediate valence regime, especially in the spin-polarized regime where the effective degeneracy is smaller. Consequently, we conclude that the hopping t strongly reduces the peak of the quadrupolar susceptibility in the Kondo regime for both- the zero-magnetic-field and the spin-polarized situations. As seen in figures 1(D) and 2(D) the slope of $\ln \chi_{quadr}$ with ϵ_{e_g} in the Kondo regime is asymptotically the same independently of t, but the prefactor is strongly reduced with t, especially in the ferromagnetic regime. This trend is reversed for $\epsilon_{e_g} > 0$ (the perturbative regime in powers of V) because increasing t enhances the occupation of the bonding level as compared to $t = 0$. The linear response to the quadrupolar splitting of the e_g levels is related to the coupling of the ions to the lattice (Jahn–Teller effect) and hence to the effective Mn–O–Mn bond lengths and angles. The present approach indicates that t suppresses these lattice distortions.

Also the peak in the charge susceptibility in the intermediate valent region and the response function for charge imbalance between sites are strongly reduced by the intersite hopping in both zero magnetic field and for the ferromagnetic lattice. Since the area under the charge susceptibility is normalized to one, a reduction of the peak automatically implies an enhancement in the tails. The charge imbalance response function basically tracks the trends of the charge susceptibility. These quantities are a measure of the potential for charge order in a lattice of Mn ions and the formation of small polarons. It is still an open question whether the coherence in the lattice reverses this trend in accordance with the experimental observations.

Acknowledgments

The support by the US Department of Energy under grant No DE-FG02-98ER45707 and by the US National Science Foundation under grant DMR98-01751 is acknowledged.

References

[1] Jin S, McCormack M, Tiefel T H, Fleming R H, Phillips J and Ramesh R 1994 *Science* **264** 413
[2] Jonker G H and van Santen J H 1950 *Physica* **16** 337

Jonker G H 1956 *Physica* **22** 707
Wollan E O and Koehler W C 1955 *Phys. Rev.* **100** 545
[3] v. Helmolt R, Wecker J, Holzapfel B, Schultz L and Samwer K 1993 *Phys. Rev. Lett.* **71** 2331
Chahara K, Ohuo T, Kasai M and Kozono Y 1993 *Appl. Phys. Lett.* **63** 1990
Xiong G C *et al* 1995 *Apl. Phys. Lett.* **66** 1427
Tokura Y *et al* 1994 *J. Phys. Soc. Japan* **63** 3931
[4] Zhao G, Conder K, Keller H and Müller K A 1996 *Nature* **381** 676
[5] Millis A J, Shraiman B I and Mueller R 1996 *Phys. Rev. Lett.* **77** 175
[6] Snyder G J, Hiskes R, DiCarolis S, Beasley M R and Geballe T H 1996 *Phys. Rev.* B **53** 14 434
[7] Booth C H, Bridges F, Snyder G J and Geballe T H 1997 *Phys. Rev.* B **54** 15 606
Billinge S J L, DiFrancesco R G, Kwei G H, Neumeier J J and Thompson J D 1996 *Phys. Rev. Lett.* **77** 715
[8] Millis A J, Littlewood P B and Shraiman B I 1995 *Phys. Rev. Lett.* **74** 5144
Furukawa N 1995 *J. Phys. Soc. Japan* **64** 2734
Röder H, Jun Zang and Bishop A R 1997 *Phys. Rev. Lett.* **76** 1356
[9] Goodenough J 1955 *Phys. Rev.* **100** 564
[10] Schlottmann P and Lee K 1997 *Phys. Rev.* B **56** 13 999
[11] Schlottmann P 1997 *Phil. Mag. Lett.* **76** 435
[12] Schlottmann P 1998 *Phys. Rev.* B **57** 10 630
[13] Schlottmann P 1998 *Phys. Rev.* B **58** 3160
[14] Zener C 1951 *Phys. Rev.* **82** 403
Anderson P W and Hasegawa H 1955 *Phys. Rev.* **100** 675
de Gennes P G 1960 *Phys. Rev.* **118** 141
[15] Mazzaferro J, Balseiro C A and Alascio B 1981 *Phys. Rev. Lett.* **47** 274
[16] Schlottmann P 1982 *Valence Instabilities* ed P Wachter and H Boppart (Amsterdam: North-Holland) p 471
[17] Bickers N E 1987 *Rev. Mod. Phys.* **59** 845
[18] Jayaprakash C, Krishnamurthy H R and Wilkins J W 1981 *Phys. Rev. Lett.* **47** 737
[19] Barnes S E 1976 *J. Phys. F: Met. Phys.* **6** 1375
Coleman P 1984 *Phys. Rev.* B **29** 3035
[20] Read N and Newns D M 1983 *J. Phys. C: Solid State Phys.* **16** L1055
Coleman P 1985 *J. Magn. Magn. Mater.* **47** 323
[21] Coleman P 1985 *Theory of Heavy Fermions and Valence Fluctuations* ed T Kasuya and T Saso (New York: Springer) p 163
[22] Millis A J and Lee P A 1987 *Phys. Rev.* B **35** 3394
Auerbach A and Levin K 1986 *Phys. Rev. Lett.* **57** 877
[23] Dorin V and Schlottmann P 1992 *Phys. Rev.* B **46** 10 800
Dorin V and Schlottmann P 1993 *Phys. Rev.* B **47** 5095